Glass Formation and Soft Magnetic Properties of Partially Co-substituted $Fe_{71-x}Nb_6B_{23}Co_x$ Glassy Alloys

Li-Juan YAO[1,a,*], Zeng-Yun JIAN[1,b], Man ZHU[1,c], Rui-Hua NAN[1,d], Chang-Qin JIN[1,e] and Fang-E CHANG[1,f]

[1]School of Materials and Chemical Engineering, Xi'an Technological University, Xi'an, Shaanxi 710021, P. R. China

[a]ylj8453@126.com, [b]jianzengyun@xatu.edu.cn, [c]zhuman0428@126.com, [d]20733575@qq.com, [e]553465077@qq.com, [f]cfe.ch@163.com

Keywords: Metallic glasses, Glass forming ability, Differential scanning calorimetry, Magnetic properties

Abstract. The influence of partial substitution of Fe by Co on the glass forming ability and soft magnetic properties of the $Fe_{71-x}Nb_6B_{23}Co_x$ (x=1, 2, 3, 4) metallic glasses were investigated using X-ray diffraction (XRD), differential scanning calorimetry (DSC), and vibrating sample magnetometer (VSM). These glassy alloys exhibit high thermal stability and large glass forming ability (GFA). The supercooled liquid region ΔT_x, T_{rg}, and γ for $Fe_{71-x}Nb_6B_{23}Co_x$ metallic glasses are equal to 50–63 K, 0.584–0.592, and 0.391–0.400, respectively. Magnetization measurement indicates that the saturation magnetization ranges from 94 to 113 emu/g for the $Fe_{71-x}Nb_6B_{23}Co_x$ glassy alloys. As Co content increases from 1 at.% to 4 at.%, thermal stability, GFA, and saturation magnetization are decreased. The $Fe_{70}Nb_6B_{23}Co_1$ glassy alloy is found to have the largest GFA with a maximum ΔT_x of 63 K and good soft magnetic properties with high saturation magnetization. The $Fe_{71-x}Nb_6B_{23}Co_x$ glassy alloys can be served as a good candidate for soft magnetic materials because of large GFA, good soft magnetic properties and low cost of raw materials.

1. Introduction

Fe–based metallic glasses have received great attention due to their high yield strength, good corrosion resistance, and good processability within supercooled liquid region [1-3]. These glassy alloys were widely used in engineering field, such as, magnetic core, switch transformer, and electronic micro-components, due to their abundant natural resources, low material cost, and excellent soft magnetic properties.

Since the first soft magnetic material in Fe–C–P alloy system reported by Duwez *et al*. [4], great endeavor has been devoted to the development of new Fe-based metallic glasses [5-8]. Among these glass-formers, the ternary Fe–Nb–B alloy system has been intensively studied. The glass formation, structure, and the magnetic properties of glassy ribbons in Fe–Nb–B alloy system have been studied [6, 7, 9, 10]. Nanocrystalline Fe–Nb–B ternary alloys were fabricated by annealing the these glassy ribbons. Makino *et al*. [9] reported that saturation magnetization of nanocrystalline $Fe_{84}Nb_7B_9$ alloy reaches 1.49 *T*. Stoica *et al*. [11] reported a ternary $Fe_{66}Nb_4B_{30}$ bulk metallic glass (BMG) with a critical diameter of 2 mm in the high-boron-content region of the Fe–Nb–B ternary system. The glass forming ability (GFA) in relation to microstructure evolution in the Fe–Nb–B ternary alloy was investigated in detail by Yao *et al*. [12, 13]. In order to improve the GFA as well as soft magnetic property, many attempts were devoted to the development of Fe–Nb–B alloy system by introducing minor amount of Y [6, 14], Zr [6], Ni [7], and Co [15] elements.

As a staring alloy composition, we selected $Fe_{71}Nb_6B_{23}$ glassy alloys since high GFA (a maximum diameter up to 1.5 mm) coupled with ultrahigh strength has been reported [12]. A series of quaternary $Fe_{71-x}Nb_6B_{23}Co_x$ (x=1, 2, 3, 4) alloys were developed. In present study, the effect of partial substitution of Fe by Co on the thermal stability, structure and magnetic properties in the Fe–Nb–B–Co quantary alloys was investigated. It was found that upon substitution, the thermal

stability becomes better, with a glass transition temperature exceeding 835 K and with a maximum extension of supercooled liquid region reaching 63 K for alloy $Fe_{70}Nb_6B_{23}Co_1$.

2. Experimental Procedure

Alloy ingots with nominal composition of $Fe_{71-x}Nb_6B_{23}Co_x$ (x=1, 2, 3, 4) were arc-melted using purity elements of Fe (99.8 wt%), Nb (99.8 wt%), Co (99.8 wt%), and Fe-17.5 wt%B master alloy in the Ti-gettered argon atmosphere. During this process, the alloy ingots were re-melted for six times in order to ensure the compositional homogeneity. The melt-spun ribbons were prepared by injecting the molten alloys contained in a quartz tube into a single copper roller with a linear velocity of 40 m/s and ejection pressure of 20 kPa under the argon protective atmosphere. The ribbons have a thickness of 20–30 μm and a width of 2–4 mm. The amorphous structure of the melt-spun ribbons was identified by X-ray diffraction (XRD; Bruker D8 advance) with Cu Kα radiation. Thermal behaviors of these samples were measured using differential scanning calorimetry (DSC; Mettler-Toledo TGA/DSC1) at a heating rate of 0.67 K s^{-1}. The DSC result for each sample was examined for three times, and the errors of characteristic temperatures are within ±3 K. The magnetic properties were measured using a vibrating sample magnetometer (VSM) under a maximum applied magnetic field of 10, 000 Oe.

3. Results and Discussion

3.1. Structural Characterization

Fig. 1 shows the XRD patterns taken from the melt–spun ribbons of $Fe_{71-x}Nb_6B_{23}Co_x$ alloy system. All the XRD patterns exhibit a broad diffuse peak in the 2θ range 35º–55º without any detectable sharp Bragg peaks, indicating the formation of a fully amorphous state in all these samples with different Co contents.

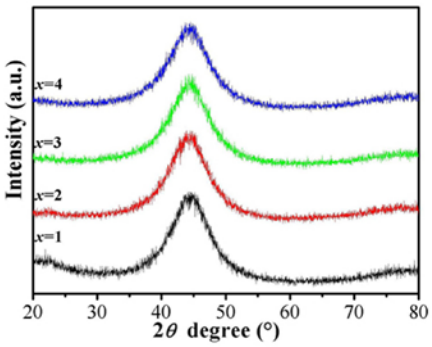

Fig. 1 XRD patterns of the melt-spun $Fe_{71-x}Nb_6B_{23}Co_x$ (x=1, 2, 3, 4) alloys.

3.2. Glass Forming Ability of $Fe_{71-x}Nb_6B_{23}Co_x$ alloys

Fig. 2 illustrates the DSC traces taken from the melt-spun $Fe_{71-x}Nb_6B_{23}Co_x$ (x=1, 2, 3, 4) ribbons at a constant heating rate of 0.67 K s^{-1}. From Fig. 2a, it is observed that each alloy exhibits a distinct glass transition followed by a wide supercooled liquid region before crystallization events. Table 1 lists the glass transition temperature T_g, onset crystallization temperatures T_{x1} and T_{x2}, melting temperature T_m, liquidus temperature T_l, the suprecooled liquid region ΔT_x, and other GFA parameters T_{rg} and γ. Each of the traces has two distinct exothermic peaks, demonstrating the crystallization processes include two stages. The temperature intervals between T_{x1} and T_{x2} are in the range 190–220 K. With increasing Co content from 1 at.% to 4 at.%, the values of T_g and T_{x1} decreases from 852 K to 835 K, and from 915 K to 885 K, respectively, and the corresponding ΔT_x (=T_{x1}–T_g) is also found to gradually decrease from 63 K to 50 K. A maximum ΔT_x value of 63 K can be achieved for alloys with

x=1. Therefore, as the Co content in the alloy increases, the thermal stability and the GFA are decreased.

The melting behavior of the present alloys was also measured, and the results were shown in Fig. 2b. Only single endothermic peak can be detected for all the compositions with different Co contents, and the values of T_m and T_l are in the range 1393–1401 K and 1424–1438 K, respectively. This phenomenon implies that the substitution of appropriate amount of Co can make the alloy composition approach to a eutectic point, which is in accordance with that reported by Zhao *et al*. [16]. Other GFA parameters, T_{rg} (=T_g/T_l) and γ (=$T_{x1}/(T_g+T_l)$), were also estimated. It is found that partial substitution of Fe by Co results in a continuous decrease of T_{rg} from 0.592 to 0.584, and γ from 0.400 to 0.391, respectively. The thermal stability and GFA of present $Fe_{71-x}Nb_6B_{23}Co_x$ glassy alloys are superior to that of $Fe_{71}Nb_6B_{23}$ BMG [12]. The $Fe_{70}Nb_6B_{23}Co_1$ alloys can be considered as the best glass former with high thermal stability against crystallization and the optimum GFA. An excessive addition of Co element deteriorates the GFA of the alloy system due to the precipitation of primary α–(Fe, Co) crystalline phase [17].

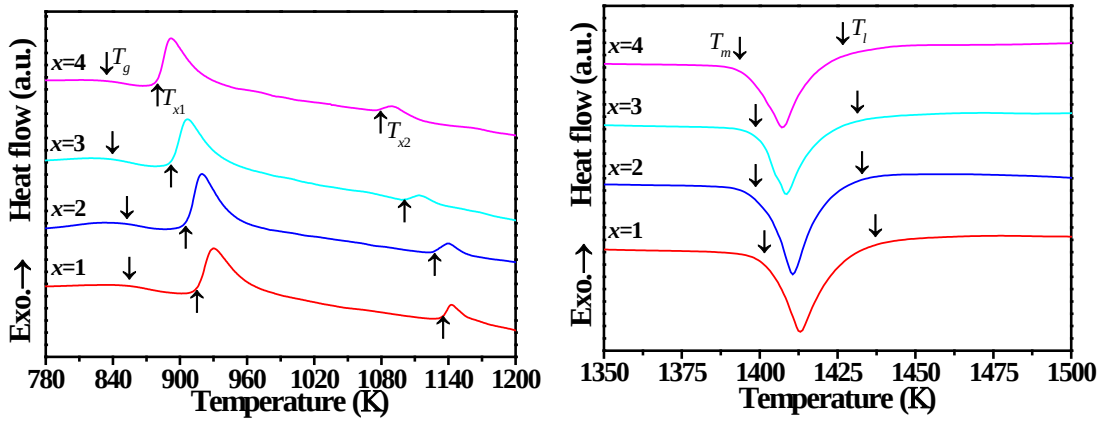

Fig. 2 DSC traces of the melt-spun $Fe_{71-x}Nb_6B_{23}Co_x$ (x=1, 2, 3, 4) ribbons at a constant heating rate of 0.67 K s^{-1}. (a) glass transition and crystallization behaviors; and (b) melting behavior.

Table 1 Thermal properties and the calculated thermodynamic parameters of the FeNbBCo glassy alloys.

Materials	Measured thermal properties								Thermodynamic parameters		
	T_g (K)	T_{x1} (K)	T_{x2} (K)	T_m (K)	T_l (K)	ΔT_x (K)	T_{rg}	γ	δ	ΔH_{mix} (kJ/mol)	ΔS_{mix} (kJ/mol/K)
$Fe_{70}Nb_6B_{23}Co_1$	852	915	1135	1401	1438	63	0.592	0.400	16.32	–11.40	6.67
$Fe_{69}Nb_6B_{23}Co_2$	848	906	1125	1400	1434	58	0.591	0.397	16.33	–11.41	6.99
$Fe_{68}Nb_6B_{23}Co_3$	837	894	1102	1398	1424	57	0.588	0.395	16.33	–11.41	7.27
$Fe_{67}Nb_6B_{23}Co_4$	835	885	1075	1393	1426	50	0.584	0.391	16.34	–11.42	7.51

In order to explain the thermal stability and GFA in the multi-component alloys, three parameters including atomic size difference (δ), the mixing enthalpy (ΔH_{mix}), and the mixing entropy (ΔS_{mix}) [18], were used to characterize the collective behavior of the constitute elements. These three parameters were defined by Eqs. (1–3), respectively.

$$\delta = 100\sqrt{\sum_{i=1}^{n} c_i\left(1-r_i/r\right)^2} \tag{1}$$

where, $r = \sum_{i=1}^{n} c_i r_i$ represents average atomic radius, c_i and r_i are the atomic fraction and atomic radius of the ith element, respectively.

$$\Delta H_{\text{mix}} = \sum_{i=1, i\neq j}^{n} \Omega_{ij} c_i c_j \tag{2}$$

where, $\Omega_{ij} = 4\Delta H_{\text{mix}}^{\text{AB}}$ and $\Delta H_{\text{mix}}^{\text{AB}}$ is the mixing enthalpy of binary liquid A-B alloys.

$$\Delta S_{\text{mix}} = -R\sum_{i=1}^{n} c_i \ln c_i \tag{3}$$

where, R is the gas constant.

The calculated values of δ, ΔH_{mix}, and ΔS_{mix} were also listed in Table 1. It can be seen that δ is larger than 16.32 and ΔH_{mix} is less than –11.42 kJ/mol. The calculated values of δ and ΔH_{mix} are almost the same for alloys with different Co contents. The ΔS_{mix} value increases from 6.67 to 7.51 kJ/(mol·K) with increasing Co content.

The reason for large GFA of the FeNbBCo glassy alloys is believed to result from the satisfaction of the empirical rules suggested by Inoue *et al*. [19]. First, Fe–Nb–B–Co alloys consist of four components. On the basis of the "confusion principle" suggested by Greer [20], the more elements involved, the lower the chance that the alloy can select viable crystal structures, and the greater the chance of glass formation. Second, the atomic size of the adopted elements decreases in the order of Nb(0.14290 nm) > Co(0.12510 nm) > Fe(0.12412 nm) > B(0.08200 nm) [21]. There is significant difference in atomic size ratio among the main constituent elements. The atomic size difference δ is larger than 16.32. Third, negative heats of mixing among the main constituent elements should exist. Mixing enthalpies of the main constituent elements for Fe–Nb, Fe–B, and Nb–B pairs are –16, –11, and –27 kJ/mol, respectively. Co and Fe have a very moderately negative mixing enthalpy of –1 kJ/mol, whereas the other constituent elements have stronger negative values (e.g., Co–Nb: –25 kJ/mol, and Co–B: –9 kJ/mol) [22]. The negative mixing enthalpy of the Co–Nb pair is larger than that of the Fe–Nb and Fe–B pairs. The large atomic size difference (δ>16) and large negative enthalpy (ΔH_{mix}<–11 kJ/mol) of the $Fe_{71-x}Nb_6B_{23}Co_x$ (x=1, 2, 3, 4) alloys (Table 1) account for their good thermal stability in the undercooled liquid state. The large atoms (Co) and small atoms (B) may strengthen the "backbone" in the amorphous structure and the degree of close–packed structure. It is believed that replacing Fe with Co would increase the atomic packing density of the liquid structure and cause the suppression of nucleation of crystalline phases, thus resulting in an improvement of the GFA.

3.3. Soft Magnetic Properties

Fig. 3 shows room temperature magnetic hysteresis loops (M–H) of the melt-spun $Fe_{71-x}Nb_6B_{23}Co_x$ (x=1, 2, 3, 4) alloys, and the insert displays the relationship between saturation magnetization (M_s) and coercivity (H_c) and Co content. Present glassy alloys exhibit typical of a soft magnetic material. The M_s value reaches 113 emu/g for alloys with x=1. The M_s value decreases from 113 to 94 emu/g with increasing Co content. And the H_c ranges from 5.4 to 10.9 Oe for the melt-spun $Fe_{71-x}Nb_6B_{23}Co_x$ (x=1, 2, 3, 4) alloys. In present FeNbBCo alloy system, Fe and Co are ferromagnetic elements, while Nb and B are non-magnetic in nature. The electron configuration of Co atom is almost the same as that of Fe atom, and their magnetization derives from the spin polarization of the itinerant d electrons. Fe is magnetically weak, while Co is magnetically saturated. The 3d bands of Fe atom are divided into 3d spin-up electrons and 3d spin-down electrons. The occupation numbers of the spin-up and the spin-down in the spin-polarized d band for Fe and Co are 4.4, 2.2, and 4.6, 2.9, respectively [23]. Although the reason for the variation of the saturation magnetization is not well understood, partial substitution of Fe by Co would affect the local magnetic moment because it may modify the atomic environment around the Fe atoms [24]. Because the negative mixing enthalpy of Co–Nb pairs is

larger than that of Fe–Nb, and Fe–B pairs, Nb will preferentially locate around Co atoms. Partial replacement of Fe by Co may decrease the difference between spin-up and the spin-down 3*d* band [25], thus decreasing the average magnetic moment of the $Fe_{71-x}Nb_6B_{23}Co_x$ glassy alloys.

The H_c value depends mostly on surface and pinning effect of magnetic domain walls. Due to surface irregularities, the H_c value is proportional to the ratio of the surface roughness amplitude to the specimen thickness. This contribution to H_c should be high for ribbons, because the surface after casting is not very smooth and its width is several orders of magnitude larger than the thickness [11]. Besides, the contribution of pinning effect to H_c is related to the existence of inclusions in the alloys. These inclusions mainly come from the industrial grade raw materials, and they would act as pinning sites for magnetic domain walls inside amorphous alloys [26], thus consequently inducing a higher coercivity. It is concluded that the Fe–Nb–B–Co amorphous ribbons are promising for potential application as new functional materials due to their superior magnetic properties, large GFA and low cost of raw materials.

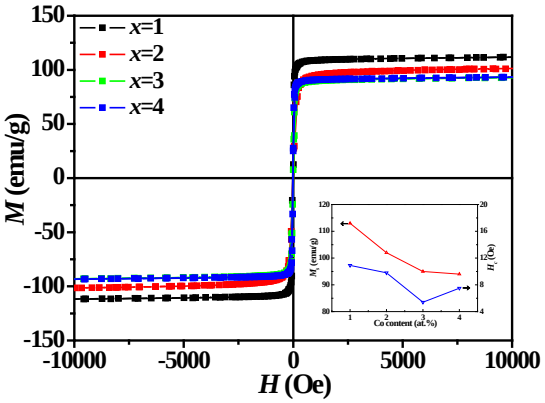

Fig. 3 Room-temperature magnetic hysteresis loops (*M–H*) for the melt-spun $Fe_{71-x}Nb_6B_{23}Co_x$ (x=1, 2, 3, 4) alloys, and the insert showing the variation of the saturation magnetization and coercivity with Co content.

4. Summary

The effect of Co substitution for Fe on the glass forming ability and soft magnetic properties was studied. The Co content in the alloys is a determination factor affecting the GFA and soft magnetic properties. The substitution of Fe by an appropriate amount of Co decreases both thermal stability and GFA of the $Fe_{71-x}Nb_6B_{23}Co_x$ glassy alloys. The $Fe_{70}Nb_6B_{23}Co_1$ glassy alloy reveals larger GFA and high thermal stability with a maximum ΔT_x of 63 K and T_{x1} of 915 K. Additionally, these $Fe_{71-x}Nb_6B_{23}Co_x$ glassy alloys exhibit excellent soft magnetic properties with high saturation magnetization of 94–113 emu/g and low coercivity of 5.4–10.9 Oe. The combination of good soft magnetic properties, large GFA and low cost of raw materials makes present FeNbBCo glassy alloys a good candidate for soft magnetic materials.

Acknowledgement

This work was supported by the National Natural Science Foundation of China (Grant nos. 51301125, 51171136, 51502234, 11404251), Scientific Research Program Funded by Shaanxi Provincial Education Department (Grant nos. 2013JK0907), and the fund of the State Key Laboratory of Solidification Processing in NWPU (Grant no. SKLSP201410).

References

[1] A. Inoue, Acta Mater. 48 (2000) 279–306.

[2] S.Y. Meng, H.B. Ling, Q. Li, J.J. Zhang, Scripta Mater. 81 (2014) 24–27.

[3] C.Y. Lin, H.Y. Tien, T.S. Chin, Appl. Phys. Lett. 86 (2005) 162501.

[4] P. Duwez, S.C.H. Lin, J. Appl. Phys. 38 (1967) 4096–4097.

[5] Z.P. Lu, C.T. Liu, J.R. Thompson, W.D. Porter, Phys. Rev. Lett. 92 (2004) 245503.

[6] J.M. Park, J.S. Park, D.H. Kim, J.H. Kim, J. Mater. Res. 21 (2006) 1019–1024.

[7] J.M. Park, G. Wang, R. Li, N. Mattern, J. Eckert, D.H. Kim, Appl. Phys. Lett. 96 (2010) 031905.

[8] J.W. Li, H. Men, B.L. Shen, AIP Advances 1 (2011) 042110.

[9] A. Makino, K. Suzuki, A. Inoue, T. Masumoto, Mater. Sci. Engin. A A179/180 (1994) 127–131.

[10] J. Torrens-Serra, J. Rodríguez-Viejo, M. T. Clavaguera-Mora, Phy. Rev. B 76 (2007) 214111.

[11] M. Stoica, K. Hajlaoui, A. Lemoulec, A.R. Yavari, Philo. Mag. Lett. 86 (2006) 267–275.

[12] J.H. Yao, J.Q. Wang, Y. Li, Appl. Phys. Lett. 92 (2008) 251906.

[13] J.H. Yao, H. Yang, J. Zhang, J.Q. Wang, Y. Li, J. Mater. Res. 23 (2008) 392–401.

[14] D.S. Song, J.H. Kim, E. Fleury, W.T. Kim, D.H. Kim, J. Alloys Compd. 389 (2005) 159–164.

[15] Z.Y. Chang, X.M. Huang, L.Y. Chen, M.Y. Ge, Q.K. Jiang, X.P. Nie, J.Z. Jiang, Mater. Sci. Engin. A 517 (2009) 246–248.

[16] C.L. Zhao, C.C. Dun, Q.K. Man, B.L. Shen, Intermetallics 32 (2013) 408–412.

[17] S.F. Guo, Z.Y. Wu, L. Liu, J. Alloys Compd. 468 (2009) 54–57.

[18] S. Guo, C.T. Liu, Prog. Nat. Sci.: Mater. Int. 21(2011) 433−446.

[19] A. Takeuchi, A. Inoue, Mater. Trans. 42 (2005) 2817–2829.

[20] A.L. Greer, Nature 336 (1993) 303–304.

[21] O.N. Senkov, D.B. Miracleb, Mater. Res. Bull. 36 (2001) 2183–2198.

[22] de Boer FR, Boom R, Mattens WCM, Miedema AR, Niessen AK. In: de Boer FR, Pettifor DG, editors. Cohesion and structure, vol. 1. Amsterdam: North Holland Physics, (1988).

[23] P. Soderlind, R. Ahuja, O. Eriksson, J.M. Wills, B. Johansson, Phy. Rev. B, 50 (1994) 5918–5927.

[24] R.S. Sundar, S.C. Deevi, Inter. Mater. Rev. 50 (2005) 157–192.

[25] R. H. Victora and L. M. Falicov, S. Ishida, Phy. Rev. B 30 (1984) 3896–3902.

[26] H.X. Li, J.E. Gao, S.L. Wang, S. Yi, Z.P. Lu, Metall. Mater. Trans. A 43 (2012) 2615–2619.

